

POLYTOPAL SCHEMES FOR FLOWS IN FRACTURED POROUS MEDIA

Jérôme Droniou

joint works with R. Masson, A. Haidar, G. Enchéry and I. Faille.

IMAG, CNRS, France,
School of Mathematics, Monash University, Australia

<https://imag.umontpellier.fr/~droniou/>

ICOSAHOM 2025, 15-19 July 2025



Slides:



References for this presentation

- Design of the method, application to poromechanics with Coulomb friction:

Droniou, J., Enchéry, G., Faille, I., Haidar, A., and Masson, R. *A bubble VEM–fully discrete polytopal scheme for mixed-dimensional poromechanics with frictional contact at matrix-fracture interfaces*. Computer Methods in Applied Mechanics and Engineering, 422:116838, 2024.

<https://arxiv.org/abs/2312.09319>

- Analysis for purely mechanical model with Tresca friction:

Droniou, J., Haidar, A., and Masson, R. *Analysis of a VEM–fully discrete polytopal scheme with bubble stabilisation for contact mechanics with tresca friction*. ESAIM: M2AN Math. Model. Numer. Anal. 59 (2), pp. 1043–1074, 2025. <http://arxiv.org/abs/2404.03045>.

See also references inside.

Outline

- 1 Mixed-dimensional poromechanical model
- 2 Hybrid finite volume scheme for flow
- 3 Bubble-enriched polytopal scheme for mechanical model
- 4 Theoretical results
- 5 Numerical results
 - Contact mechanics: convergence
 - Contact mechanics: benefit of polyhedral meshes
 - 3D full poro-mechanical model

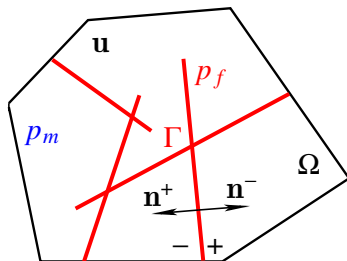
Slides:



Matrix and fracture network

Notations: Ω domain (matrix), Γ fracture, two sides \pm with outward normals \mathbf{n}^\pm .

Unknowns: displacement \mathbf{u} in matrix (discontinuous across fractures), pressure p_m in matrix, pressure p_f in fracture.



Flow equations: Darcy law for p_m , Poiseuille law for p_f .

$$\left\{ \begin{array}{ll} \partial_t \phi_m + \operatorname{div} \mathbf{V}_m = h_m & \text{on } (0, T) \times \Omega \setminus \bar{\Gamma}, \\ \mathbf{V}_m = -\frac{\mathbb{K}_m}{\eta} \nabla p_m & \text{on } (0, T) \times \Omega \setminus \bar{\Gamma}, \\ \partial_t d_f + \operatorname{div}_\tau \mathbf{V}_f - \llbracket \mathbf{V}_m \rrbracket_{\mathbf{n}} = h_f & \text{on } (0, T) \times \Gamma, \\ \mathbf{V}_f = \frac{(d_f)^3}{12\eta} \nabla_\tau p_f & \text{on } (0, T) \times \Gamma, \\ \gamma_{\mathbf{n}}^\pm \mathbf{V}_m = \frac{2\mathbf{K}_{f,\mathbf{n}}}{d_f} \llbracket p \rrbracket^\pm & \text{on } (0, T) \times \Gamma \end{array} \right.$$

with

$$\partial_t \phi_m = b \operatorname{div}(\partial_t \mathbf{u}) + \frac{1}{M} \partial_t p_m, \quad d_f = d_f^c - \llbracket \mathbf{u} \rrbracket_{\mathbf{n}}.$$

Notations: $\llbracket \mathbf{V}_m \rrbracket_{\mathbf{n}} = \gamma_{\mathbf{n}}^+ \mathbf{V}_m - \gamma_{\mathbf{n}}^- \mathbf{V}_m$, $\llbracket p \rrbracket^\pm = \gamma^\pm p_m - p_f$.

$$\boldsymbol{\sigma}(\mathbf{u}) = 2\mu\boldsymbol{\epsilon}(\mathbf{u}) + \lambda(\operatorname{div} \mathbf{u}) \mathbb{I} \quad (\text{Effective stress}),$$

$$\boldsymbol{\sigma}^\top(\mathbf{u}, p_m) = \boldsymbol{\sigma}(\mathbf{u}) - b p_m \mathbb{I} \quad (\text{Total stress}),$$

$$\mathbf{T}^\pm = \gamma_\mathbf{n}^\pm \boldsymbol{\sigma}^\top(\mathbf{u}, p_m) + p_f \mathbf{n}^\pm \quad (\text{Traction}).$$

Mechanical equations: quasi-static contact-mechanics for \mathbf{u} with Coulomb friction.

$$\left\{ \begin{array}{ll} -\operatorname{div} \boldsymbol{\sigma}^\top(\mathbf{u}, p_m) = \mathbf{f} & \text{on } (0, T) \times \Omega \setminus \overline{\Gamma}, \\ \mathbf{T}^+ + \mathbf{T}^- = 0 & \text{on } (0, T) \times \Gamma, \\ T_\mathbf{n} \leq 0, \llbracket \mathbf{u} \rrbracket_\mathbf{n} \leq 0, \llbracket \mathbf{u} \rrbracket_\mathbf{n} T_\mathbf{n} = 0, & \text{on } (0, T) \times \Gamma, \\ |\mathbf{T}_\tau| \leq -F T_\mathbf{n} & \text{on } (0, T) \times \Gamma, \\ \mathbf{T}_\tau \cdot \partial_t \llbracket \mathbf{u} \rrbracket_\tau - F T_\mathbf{n} |\partial_t \llbracket \mathbf{u} \rrbracket_\tau| = 0 & \text{on } (0, T) \times \Gamma. \end{array} \right.$$

Notations: X_τ and $X_\mathbf{n}$: tangential and normal components of \mathbf{X} along Γ .

Other contact models: no friction ($F = 0$); Tresca friction ($-F T_\mathbf{n} \rightsquigarrow g$ and $\partial_t \llbracket \mathbf{u} \rrbracket \rightsquigarrow \llbracket \mathbf{u} \rrbracket$).

Poromechanics III

Weak formulation for mechanical equations: using Lagrange multiplier $\lambda = -\mathbf{T}^+$ to impose the contact conditions.

Spaces and cone:

$$\begin{aligned} \mathbf{U}_0 &= \{\mathbf{v} \in H^1(\Omega \setminus \overline{\Gamma})^d : \mathbf{v}|_{\partial\Omega} = 0\}, \\ \mathbf{C}_f(\lambda_n) &= \left\{ \boldsymbol{\mu} \in H^{-1/2}(\Gamma)^d : \langle \boldsymbol{\mu}, \mathbf{v} \rangle_\Gamma \leq \langle F\lambda_n, |\mathbf{v}_\tau| \rangle_\Gamma \right. \\ &\quad \left. \forall \mathbf{v} \in (H^{1/2}(\Gamma))^d \text{ s.t. } v_n \leq 0 \right\}. \end{aligned}$$

Equations: find $\mathbf{u} : [0, T] \rightarrow \mathbf{U}_0$ and $\lambda : [0, T] \rightarrow \mathbf{C}_f(\lambda_n)$ s.t., for all $\mathbf{v} : [0, T] \rightarrow \mathbf{U}_0$ and $\boldsymbol{\mu} : [0, T] \rightarrow \mathbf{C}_f(\lambda_n)$,

$$\begin{aligned} \int_{\Omega} (\boldsymbol{\sigma}(\mathbf{u}) : \boldsymbol{\epsilon}(\mathbf{v}) - b p_m \operatorname{div}(\mathbf{v})) + \langle \lambda, \llbracket \mathbf{v} \rrbracket \rangle_\Gamma + \int_{\Gamma} p_f \llbracket \mathbf{v} \rrbracket_n &= \int_{\Omega} \mathbf{f} \cdot \mathbf{v}, \\ \langle \mu_n - \lambda_n, \llbracket \mathbf{u} \rrbracket_n \rangle_\Gamma + \langle \boldsymbol{\mu}_\tau - \lambda_\tau, \llbracket \partial_t \mathbf{u} \rrbracket_\tau \rangle_\Gamma &\leq 0. \end{aligned}$$

Outline

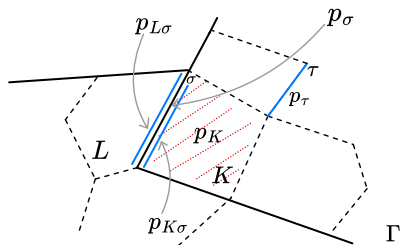
- 1 Mixed-dimensional poromechanical model
- 2 Hybrid finite volume scheme for flow
- 3 Bubble-enriched polytopal scheme for mechanical model
- 4 Theoretical results
- 5 Numerical results
 - Contact mechanics: convergence
 - Contact mechanics: benefit of polyhedral meshes
 - 3D full poro-mechanical model

Slides:



Mesh and spaces

$\mathcal{M}, \mathcal{F}, \mathcal{V}$ cells (K), faces (σ) and vertices (s). \mathcal{X}_z entities \mathcal{X} on z .



Spaces for matricial and interface pressures: $X_{\mathcal{D}} = X_{\mathcal{D}_m} \times X_{\mathcal{D}_f}$ with

$$X_{\mathcal{D}_m} = \left\{ p_{\mathcal{D}_m} = \left((p_K)_{K \in \mathcal{M}}, (p_\sigma)_{\sigma \in \mathcal{F} \setminus \mathcal{F}_T}, (p_{K\sigma})_{\sigma \in \mathcal{F}_T, K \in \mathcal{M}_\sigma} \right) : \right. \\ \left. p_K \in \mathbb{R}, p_\sigma \in \mathbb{R}, p_{K\sigma} \in \mathbb{R} \right\},$$

$$X_{\mathcal{D}_f} = \left\{ p_{\mathcal{D}_f} = \left((p_\sigma)_{\sigma \in \mathcal{F}_T}, (p_e)_{e \in \mathcal{E}_\Gamma} \right) : p_\sigma \in \mathbb{R}, p_e \in \mathbb{R} \right\}.$$

$X_{\mathcal{D}}^0$: with zero boundary conditions.

Reconstruction operators

Gradients: $\nabla_{\mathcal{D}_m} : X_{\mathcal{D}_m} \longrightarrow L^2(\Omega)^d$ such that (with $p_{K\sigma} = p_\sigma$ if $\sigma \notin \Gamma$)

$$(\nabla_{\mathcal{D}_m} p_{\mathcal{D}_m})|_K = \frac{1}{|K|} \sum_{\sigma \in \mathcal{F}_K} |\sigma| p_{K\sigma} \mathbf{n}_{K\sigma} + \text{stabilisation}.$$

Similar for $\nabla_{\mathcal{D}_f} : X_{\mathcal{D}_f} \longrightarrow L^2(\Gamma)^d$ along the fracture.

Function reconstructions: $\Pi_{\mathcal{D}_m} : X_{\mathcal{D}_m} \rightarrow L^2(\Omega)$ such that

$$(\Pi_{\mathcal{D}_m} p_{\mathcal{D}_m})|_K = p_K.$$

Similar for $\Pi_{\mathcal{D}_f} : X_{\mathcal{D}_f} \rightarrow L^2(\Gamma)$.

Jump reconstruction: $\llbracket \cdot \rrbracket^\pm : X_{\mathcal{D}} \rightarrow L^2(\Gamma)$ such that

$$(\llbracket p_{\mathcal{D}} \rrbracket^\pm)|_\sigma = p_{K\sigma} - p_\sigma \quad \text{with } K \text{ on the } \pm \text{ side.}$$

Flow scheme

Model:

$$\left\{ \begin{array}{ll} \partial_t \phi_m - \operatorname{div} \left(\frac{\mathbb{K}_m}{\eta} \nabla p_m \right) = h_m & \text{on } (0, T) \times \Omega \setminus \bar{\Gamma}, \\ \partial_t d_f - \operatorname{div}_\tau \left(\frac{(d_f)^3}{12\eta} \nabla_\tau p_f \right) - \llbracket \mathbf{V}_m \rrbracket_{\mathbf{n}} = h_f & \text{on } (0, T) \times \Gamma, \\ \gamma_{\mathbf{n}}^\pm \mathbf{V}_m = \frac{2\mathbf{K}_{f,\mathbf{n}}}{d_f} \llbracket p \rrbracket^\pm & \text{on } (0, T) \times \Gamma \end{array} \right.$$

Flow scheme

Model:

$$\begin{cases} \partial_t \phi_m - \operatorname{div} \left(\frac{\mathbb{K}_m}{\eta} \nabla p_m \right) = h_m & \text{on } (0, T) \times \Omega \setminus \bar{\Gamma}, \\ \partial_t d_f - \operatorname{div}_{\tau} \left(\frac{(d_f)^3}{12\eta} \nabla_{\tau} p_f \right) - \llbracket \mathbf{V}_m \rrbracket_{\mathbf{n}} = h_f & \text{on } (0, T) \times \Gamma, \\ \gamma_{\mathbf{n}}^{\pm} \mathbf{V}_m = \frac{2\mathbf{K}_{f,\mathbf{n}}}{d_f} \llbracket p \rrbracket^{\pm} & \text{on } (0, T) \times \Gamma \end{cases}$$

HFV scheme: Find $(p_{\mathcal{D}}^n)_{n=1,\dots,N} \in (X_{\mathcal{D}}^0)^N$ s.t., $\forall q_{\mathcal{D}} \in X_{\mathcal{D}}^0$, $\forall n = 1, \dots, N$,

$$\begin{aligned} & \int_{\Omega} \left(\delta_t^n \phi_{\mathcal{D}} \Pi_{\mathcal{D}_m} q_{\mathcal{D}_m} + \frac{\mathbb{K}_m}{\eta} \nabla_{\mathcal{D}_m} p_{\mathcal{D}_m}^n \cdot \nabla_{\mathcal{D}_m} q_{\mathcal{D}_m} \right) \\ & + \int_{\Gamma} \left(\delta_t^n d_{f,\mathcal{D}} \Pi_{\mathcal{D}_f} q_{\mathcal{D}_f} + \frac{(d_{f,\mathcal{D}}^{n-1})^3}{12\eta} \nabla_{\mathcal{D}_f} p_{\mathcal{D}_f}^n \cdot \nabla_{\mathcal{D}_f} q_{\mathcal{D}_f} \right) \\ & + \sum_{\mathbf{a} \in \{+, -\}} \int_{\Gamma} \frac{\mathbf{K}_{f,\mathbf{n}}}{d_{f,\mathcal{D}}^{n-1}} \llbracket p_{\mathcal{D}}^n \rrbracket_{\mathcal{D}}^{\mathbf{a}} \llbracket q_{\mathcal{D}} \rrbracket_{\mathcal{D}}^{\mathbf{a}} = \int_{\Omega} h_m \Pi_{\mathcal{D}_m} q_{\mathcal{D}_m} + \int_{\Gamma} h_f \Pi_{\mathcal{D}_f} q_{\mathcal{D}_f}, \end{aligned}$$

where $\delta_t^n A = \frac{A^n - A^{n-1}}{\delta t}$.

Outline

- 1 Mixed-dimensional poromechanical model
- 2 Hybrid finite volume scheme for flow
- 3 Bubble-enriched polytopal scheme for mechanical model
- 4 Theoretical results
- 5 Numerical results
 - Contact mechanics: convergence
 - Contact mechanics: benefit of polyhedral meshes
 - 3D full poro-mechanical model

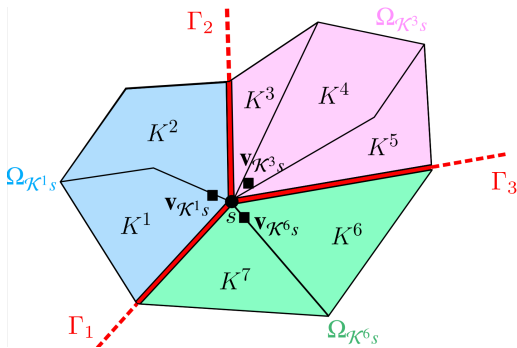
Slides:



Mesh

Polytopal mesh, compatible with fractures

- $\mathcal{F}_{\Gamma,K}^+$ faces of K on positive side of fracture.
- For $s \in \mathcal{V}$, $\mathcal{K}s$: set of cells on the same side of K .
- If $\sigma \in \mathcal{F}_{\Gamma}$: K on positive side, L on negative side.



Discrete spaces

Displacement: nodal unknowns (discontinuous across fracture) and one bubble on each fracture face (positive side).

$$\mathbf{U}_{0,\mathcal{D}} = \left\{ \mathbf{v}_{\mathcal{D}} = ((\mathbf{v}_{\mathcal{K}s})_{K \in \mathcal{M}, s \in \mathcal{V}_K}, (\mathbf{v}_{\mathbf{K}\sigma})_{K \in \mathcal{M}, \sigma \in \mathcal{F}_{\Gamma,K}^+}) : \right. \\ \mathbf{v}_{\mathcal{K}s} \in \mathbb{R}^d, \mathbf{v}_{\mathbf{K}\sigma} \in \mathbb{R}^d, \mathbf{v}_{\mathcal{K}s} = 0 \text{ if } s \in \mathcal{V}^{\text{ext}} \\ \left. \mathbf{v}_{\mathcal{K}s} = \mathbf{v}_{\mathcal{L}s} \text{ if } K, L \text{ are on the same side of } \Gamma \right\}.$$

Lagrange multipliers: piecewise constant on fracture faces.

$$\mathbf{M}_{\mathcal{D}} = \{ \lambda_{\mathcal{D}} \in L^2(\Gamma)^d : \lambda_{\sigma} := (\lambda_{\mathcal{D}})|_{\sigma} \text{ is constant for all } \sigma \in \mathcal{F}_{\Gamma} \}.$$

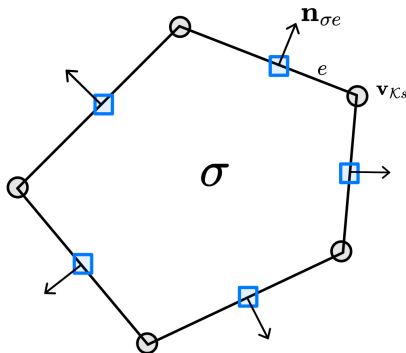
Discrete dual cone:

$$\mathbf{C}_{\mathcal{D}}(\lambda_{\mathcal{D},\mathbf{n}}) = \{ \boldsymbol{\mu}_{\mathcal{D}} = (\mu_{\mathcal{D},\mathbf{n}}, \boldsymbol{\mu}_{\mathcal{D},\tau}) \in \mathbf{M}_{\mathcal{D}} : \mu_{\mathcal{D},\mathbf{n}} \geq 0, |\boldsymbol{\mu}_{\mathcal{D},\tau}| \leq F \lambda_{\mathcal{D},\mathbf{n}} \}.$$

Reconstructions in $\mathbf{U}_{0,\mathcal{D}}$: faces

- From nodes, reconstruct edge values and use them to define the face gradient:

$$\nabla_{K\sigma} \mathbf{v}_{\mathcal{D}} = \frac{1}{|\sigma|} \sum_{e=s_1s_2 \in \mathcal{E}_\sigma} |e| \frac{\mathbf{v}_{\mathcal{K}s_1} + \mathbf{v}_{\mathcal{K}s_2}}{2} \otimes \mathbf{n}_{\sigma e}.$$



Reconstructions in $\mathbf{U}_{0,\mathcal{D}}$: faces

- From nodes, reconstruct edge values and use them to define the face gradient:

$$\nabla_{K\sigma} \mathbf{v}_{\mathcal{D}} = \frac{1}{|\sigma|} \sum_{e=s_1 s_2 \in \mathcal{E}_{\sigma}} |e| \frac{\mathbf{v}_{\mathcal{K}_{s_1}} + \mathbf{v}_{\mathcal{K}_{s_2}}}{2} \otimes \mathbf{n}_{\sigma e}.$$

- Reconstruct face averaged displacement:

$$\Pi_{K\sigma} \mathbf{v}_{\mathcal{D}} = \sum_{s \in \mathcal{V}_{\sigma}} \omega_s^{\sigma} \mathbf{v}_{\mathcal{K}_s}.$$

- Jump reconstructions, with the bubble:

$$\llbracket \mathbf{v}_{\mathcal{D}} \rrbracket_{\sigma} = \underbrace{\Pi_{K\sigma} \mathbf{v} - \Pi_{L\sigma} \mathbf{v}}_{\text{fixed by vertex DOFs}} + \underbrace{\mathbf{v}_{K\sigma}}_{\text{free}}.$$

Reconstructions in $\mathbf{U}_{0,\mathcal{D}}$: cells

Same principles...

- Using reconstructed face values **and bubble**, define the cell gradient:

$$\nabla_K \mathbf{v}_\mathcal{D} = \frac{1}{|K|} \sum_{\sigma \in \mathcal{F}_K} |\sigma| \Pi_{K\sigma} \mathbf{v} \otimes \mathbf{n}_{K\sigma} + \frac{1}{|K|} \sum_{\sigma \in \mathcal{F}_{\Gamma,K}^+} |\sigma| \mathbf{v}_{K\sigma} \otimes \mathbf{n}_{K\sigma}.$$

- Reconstruct cell averaged displacement:

$$\Pi_K \mathbf{v}_\mathcal{D} = \sum_{s \in \mathcal{V}_K} \omega_s^K \mathbf{v}_{Ks}.$$

Global reconstructions: $\llbracket \cdot \rrbracket_\mathcal{D}$, $\nabla_\mathcal{D}$, $\Pi_\mathcal{D}$, $\mathbb{E}_\mathcal{D}$, $\text{div}_\mathcal{D}$, $\mathfrak{D}_\mathcal{D}$.

Mechanics scheme

Model:

$$\int_{\Omega} (\sigma(\mathbf{u}) : \epsilon(\mathbf{v}) - b p_m \operatorname{div}(\mathbf{v})) + \langle \lambda, \llbracket \mathbf{v} \rrbracket \rangle_{\Gamma} + \int_{\Gamma} p_f \llbracket \mathbf{v} \rrbracket_n = \int_{\Omega} \mathbf{f} \cdot \mathbf{v},$$

$$\langle \mu_n - \lambda_n, \llbracket \mathbf{u} \rrbracket_n \rangle_{\Gamma} + \langle \mu_{\tau} - \lambda_{\tau}, \llbracket \partial_t \mathbf{u} \rrbracket_{\tau} \rangle_{\Gamma} \leq 0.$$

Scheme:

$$\begin{aligned} \int_{\Omega} \sigma_{\mathcal{D}}(\mathbf{u}_{\mathcal{D}}^n) : \epsilon_{\mathcal{D}}(\mathbf{v}_{\mathcal{D}}) + S_{\mu, \lambda, \mathcal{D}}(\mathbf{u}_{\mathcal{D}}^n, \mathbf{v}_{\mathcal{D}}) - \int_{\Omega} b \Pi_{\mathcal{D}_m} p_{\mathcal{D}_m}^n \operatorname{div}_{\mathcal{D}} \mathbf{v}_{\mathcal{D}} \\ + \int_{\Gamma} \Pi_{\mathcal{D}_f} p_{\mathcal{D}_f}^n \llbracket \mathbf{v}_{\mathcal{D}} \rrbracket_{\mathcal{D}, n} + \int_{\Gamma} \lambda_{\mathcal{D}}^n \cdot \llbracket \mathbf{v}_{\mathcal{D}} \rrbracket_{\mathcal{D}} = \sum_{K \in \mathcal{M}} \int_K \mathbf{f}_K^n \cdot \Pi_{\mathcal{D}} \mathbf{v}_{\mathcal{D}}, \end{aligned}$$

$$\int_{\Gamma} \left((\mu_{\mathcal{D}, n} - \lambda_{\mathcal{D}, n}^n) \llbracket \mathbf{u}_{\mathcal{D}}^n \rrbracket_{\mathcal{D}, n} + (\mu_{\mathcal{D}, \tau} - \lambda_{\mathcal{D}, \tau}^n) \cdot \llbracket \delta_t^n \mathbf{u}_{\mathcal{D}} \rrbracket_{\mathcal{D}, \tau} \right) \leq 0.$$

Note: can also be written in virtual elements framework.

Coupling equations

Model:

$$\begin{aligned}\partial_t \phi_m &= b \operatorname{div}(\partial_t \mathbf{u}) + \frac{1}{M} \partial_t p_m, \\ d_f &= d_f^c - \llbracket \mathbf{u} \rrbracket_{\mathbf{n}}.\end{aligned}$$

Discretisation:

$$\begin{aligned}\delta_t^n \phi_{\mathcal{D}} &= b \operatorname{div}_{\mathcal{D}}(\delta_t^n \mathbf{u}_{\mathcal{D}}) + \frac{1}{M} \delta_t^n \Pi_{\mathcal{D}_m} p_{\mathcal{D}_m}, \\ d_{f,\mathcal{D}}^n &= d_{f,\mathcal{D}}^c - \llbracket \mathbf{u}_{\mathcal{D}}^n \rrbracket_{\mathcal{D},\mathbf{n}},\end{aligned}$$

Outline

- 1 Mixed-dimensional poromechanical model
- 2 Hybrid finite volume scheme for flow
- 3 Bubble-enriched polytopal scheme for mechanical model
- 4 Theoretical results**
- 5 Numerical results
 - Contact mechanics: convergence
 - Contact mechanics: benefit of polyhedral meshes
 - 3D full poro-mechanical model

Slides:



On the fully coupled system

Theorem (Discrete energy estimate)

For all $n = 1, \dots, N$,

$$\begin{aligned} & \delta_t^n \int_{\Omega} \frac{1}{2} \left(\mathfrak{e}_{\mathcal{D}}(\mathbf{u}_{\mathcal{D}}) : \mathfrak{e}_{\mathcal{D}}(\mathbf{u}_{\mathcal{D}}) + S_{\mu, \lambda, \mathcal{D}}(\mathbf{u}_{\mathcal{D}}, \mathbf{u}_{\mathcal{D}}) + \frac{1}{M} |\Pi_{\mathcal{D}_m} p_{\mathcal{D}_m}|^2 \right) \\ & + \int_{\Gamma} F \lambda_{\mathcal{D}, \mathbf{n}}^n |[\![\delta_t^n \mathbf{u}_{\mathcal{D}}]\!]_{\mathcal{D}, \tau}| \\ & + \int_{\Omega} \frac{\mathbb{K}_m}{\eta} \nabla_{\mathcal{D}_m} p_{\mathcal{D}_m}^n \cdot \nabla_{\mathcal{D}_m} p_{\mathcal{D}_m}^n + \int_{\Gamma} \frac{(d_{f, \mathcal{D}}^{n-1})^3}{12\eta} |\nabla_{\mathcal{D}_f} p_{\mathcal{D}_f}^n|^2 \\ & + \sum_{\mathbf{a} \in \{+, -\}} \int_{\Gamma} \frac{\mathbf{K}_{f, \mathbf{n}}}{d_{f, \mathcal{D}}^{n-1}} ([\![p_{\mathcal{D}}^n]\!]_{\mathcal{D}}^{\mathbf{a}})^2 \\ & \leq \int_{\Omega} h_m \Pi_{\mathcal{D}_m} p_{\mathcal{D}_m}^n + \int_{\Gamma} h_f \nabla_{\mathcal{D}_f} p_{\mathcal{D}_f}^n + \sum_{K \in \mathcal{M}} \int_K \mathbf{f}_K^n \cdot \Pi_{\mathcal{D}} \delta_t^n \mathbf{u}_{\mathcal{D}}. \end{aligned}$$

Moreover, $d_{f, \mathcal{D}}^n \geq d_{f, \mathcal{D}}^c$.

On the pure mechanical model with Tresca friction

Theorem (Error estimate for Tresca)

If $\mathbf{u} \in H^2(\mathcal{M})$ and $\lambda \in H^1(\mathcal{F}_\Gamma)$, then

$$\|\nabla_{\mathcal{D}} \mathbf{u}_{\mathcal{D}} - \nabla \mathbf{u}\|_{L^2(\Omega \setminus \bar{\Gamma})} + \|\lambda_{\mathcal{D}} - \lambda\|_{-1/2, \Gamma} \lesssim C_{\mathbf{u}, \lambda} h_{\mathcal{D}}.$$

- $\|\cdot\|_{-1/2, \Gamma}$ discrete $H^{-1/2}$ -like seminorm.
- Error analysis based on **consistency** and **stability**.

Tools: Körn inequality and **inf-sup** conditions, ensured by the **bubble degrees of freedom**.

Tools: Korn and inf-sup

Discrete H^1 -norm:

$$\|\mathbf{v}_\mathcal{D}\|_{1,\mathcal{D}}^2 := \|\nabla_\mathcal{D} \mathbf{v}_\mathcal{D}\|_{L^2(\Omega)}^2 + \sum_{K \in \mathcal{M}} S_K(\mathbf{v}_\mathcal{D}, \mathbf{v}_\mathcal{D}).$$

Theorem (Discrete Korn inequality)

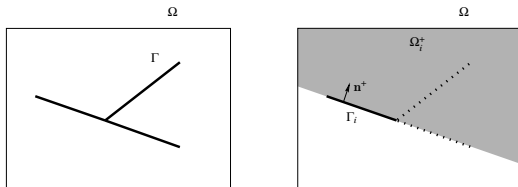
For all $\mathbf{v} \in \mathbf{U}_{0,\mathcal{D}}$,

$$\|\mathbf{v}_\mathcal{D}\|_{1,\mathcal{D}}^2 \lesssim \|\epsilon_\mathcal{D}(\mathbf{v}_\mathcal{D})\|_{L^2(\Omega)}^2 + \sum_{K \in \mathcal{M}} S_K(\mathbf{v}_\mathcal{D}, \mathbf{v}_\mathcal{D}).$$

Theorem (Discrete inf-sup condition)

$$\sup_{\mathbf{v}_\mathcal{D} \in \mathbf{U}_{0,\mathcal{D}} \setminus \{0\}} \frac{\int_\Gamma \lambda_\mathcal{D} \cdot \llbracket \mathbf{v}_\mathcal{D} \rrbracket_\mathcal{D}}{\|\mathbf{v}_\mathcal{D}\|_{1,\mathcal{D}}} \gtrsim \|\lambda_\mathcal{D}\|_{-1/2,\Gamma} \quad \forall \lambda_\mathcal{D} \in \mathbf{M}_\mathcal{D}.$$

Ideas for discrete inf-sup property I



$$\|\lambda_{\mathcal{D}}\|_{-1/2,\Gamma} := \sum_{i \in I} \sup_{\mathbf{v}_i \in H^1(\Omega_i^+; \Gamma_i)^d \setminus \{0\}} \frac{\int_{\Gamma_i} \lambda_{\mathcal{D}} \cdot \mathbf{v}_i}{\|\mathbf{v}_i\|_{H^1(\Omega_i^+)}}.$$

Ingredients for inf-sup:

- Clément-like H^1 -stable interpolator **adapted to fractures**.
- Fortin property for jump: for $\mathbf{v}_i \in H^1(\Omega_i^+; \Gamma_i)$ and $\mathbf{v}_{\mathcal{D}}$ = interpolant of extension by 0 of \mathbf{v}_i by 0,

$$\int_{\Gamma} \lambda_{\mathcal{D}} \cdot \llbracket \mathbf{v}_{\mathcal{D}} \rrbracket_{\mathcal{D}} = \int_{\Gamma_i} \lambda_{\mathcal{D}} \cdot \mathbf{v}_i.$$

Outline

- 1 Mixed-dimensional poromechanical model
- 2 Hybrid finite volume scheme for flow
- 3 Bubble-enriched polytopal scheme for mechanical model
- 4 Theoretical results
- 5 Numerical results
 - Contact mechanics: convergence
 - Contact mechanics: benefit of polyhedral meshes
 - 3D full poro-mechanical model

Slides:



Outline

- 1 Mixed-dimensional poromechanical model
- 2 Hybrid finite volume scheme for flow
- 3 Bubble-enriched polytopal scheme for mechanical model
- 4 Theoretical results
- 5 Numerical results
 - Contact mechanics: convergence
 - Contact mechanics: benefit of polyhedral meshes
 - 3D full poro-mechanical model

Static contact (Tresca), 3D manufactured solution I

Setting:

- $\Omega = (-1, 1)^3$, $\Gamma = \{0\} \times (-1, 1)^2$.
- $g = 1$, $\mu = \lambda = 1$.
- Explicit analytical solution such that:
 - sticky-contact for $z < 0$ ($\llbracket u \rrbracket_{\mathbf{n}} = 0$, $\llbracket u \rrbracket_{\boldsymbol{\tau}} = 0$)
 - slippery-contact for $z > 0$ ($\llbracket u \rrbracket_{\mathbf{n}} = 0$, $|\llbracket u \rrbracket_{\boldsymbol{\tau}}| > 0$)
- Cartesian, tetrahedral and **generalised hexahedral** meshes.

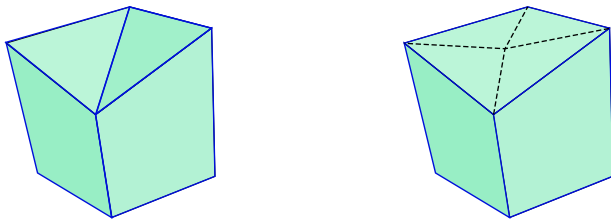
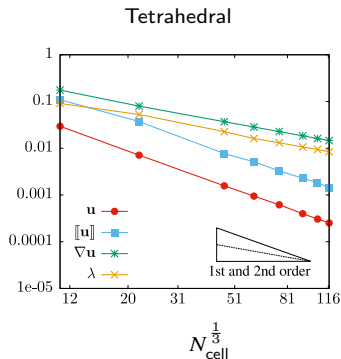
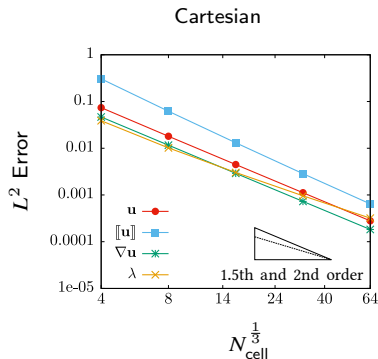


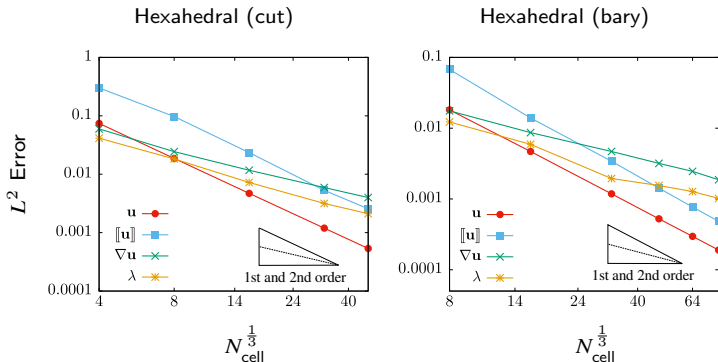
Figure: Generalised hexahedral meshes: cut (left) and barycentric subdivisions (right).

Static contact (Tresca), 3D manufactured solution II



Note: 10^{-2} accuracy for u achieved with $\sim 30^3$ Cartesian cells, $\sim 60^3$ triangular cells.

Static contact (Tresca), 3D manufactured solution III



Note: 10^{-2} accuracy for \mathbf{u} achieved with $\sim 30^3$ Hexahedral cells.

Outline

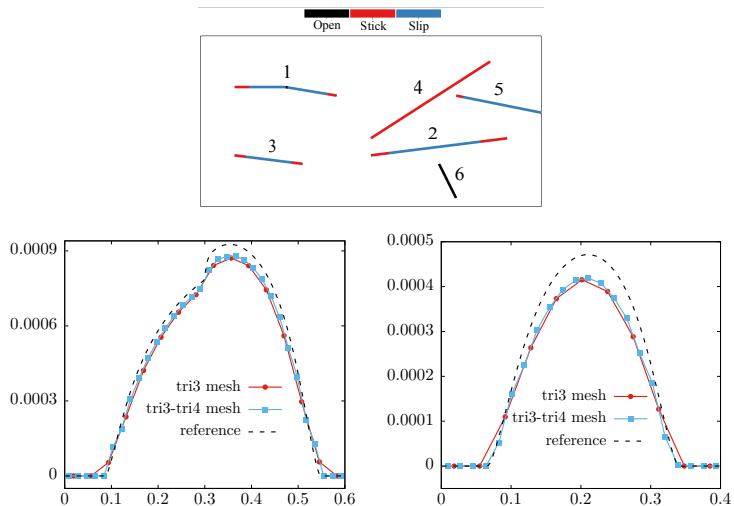
- 1 Mixed-dimensional poromechanical model
- 2 Hybrid finite volume scheme for flow
- 3 Bubble-enriched polytopal scheme for mechanical model
- 4 Theoretical results
- 5 Numerical results**
 - Contact mechanics: convergence
 - Contact mechanics: benefit of polyhedral meshes**
 - 3D full poro-mechanical model

Setting

- 6 fractures in a $2\text{m} \times 1\text{m}$ quadrangle.
- Displacement: $\mathbf{u} = 0$ at the bottom, $\mathbf{u} = [0.005\text{m}, -0.002\text{m}]$ at the top.
- $E = 4\text{GPa}$, $\nu = 0.2$, friction variable in the fractures.
- Triangular meshes, reference solution computed with 730 880 triangles.

Focus on stick-slip states of the fractures

Results



tri3: triangles.

tri3-tri4: triangles with **one additional node** at fracture edges (polygons).

Outline

- 1 Mixed-dimensional poromechanical model
- 2 Hybrid finite volume scheme for flow
- 3 Bubble-enriched polytopal scheme for mechanical model
- 4 Theoretical results
- 5 Numerical results**
 - Contact mechanics: convergence
 - Contact mechanics: benefit of polyhedral meshes
 - 3D full poro-mechanical model**

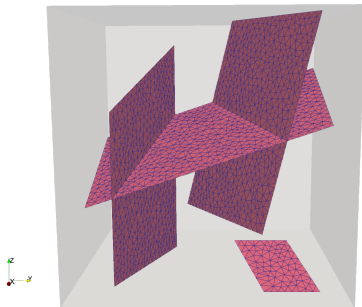
Setting

Data: $E = 4\text{GPa}$, $\nu = 0.2$, $F = 0.5$, $b = 0.5$, $M = 10\text{GPa}$.

Dirichlet BC: $\mathbf{u} = 0$ at bottom,

$$\mathbf{u}(t, x, y, 1) = \begin{cases} 0.002 \times [1, 1, -1]^\top \frac{2t}{T} & \text{if } t \leq T/2, \\ 0.002 \times [1, 1, -1]^\top & \text{if } t \geq T/2. \end{cases}$$

Fracture network:



Results I

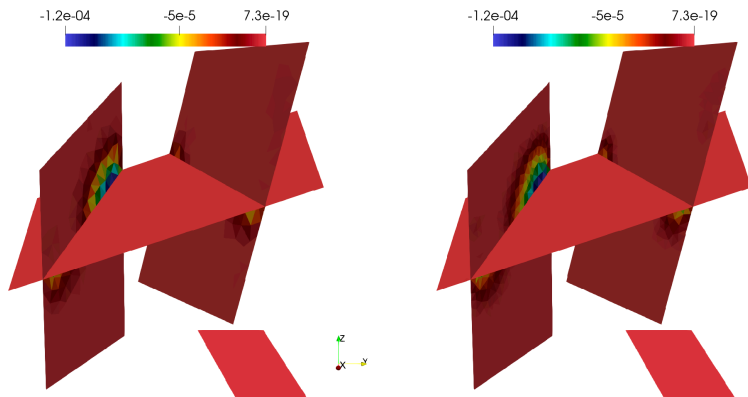


Figure: Normal displacement jumps using 47k cells (left) and 127k cells (right).

Results II

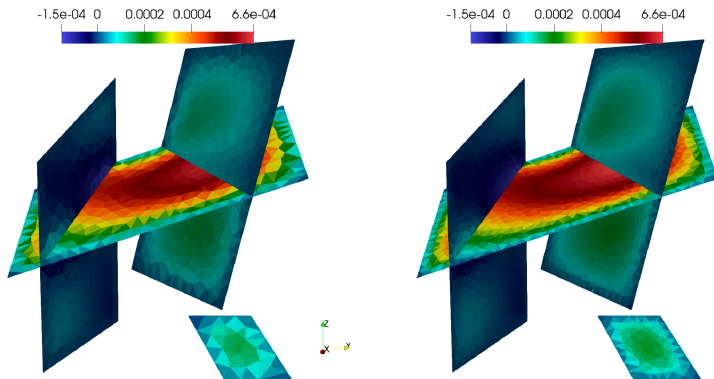


Figure: Tangential displacement jumps (one direction) using 47k cells (left) and 127k cells (right).

Conclusions

- **Polytopal** scheme, applicable on generic meshes (including hanging nodes, cut cells, local refinements). Seamlessly handles crossing fractures, etc.
- **Bubble** enrichment (first one for polytopal methods) to ensure inf-sup conditions to bound Lagrange multipliers.
- Complete **analysis** for mechanical models.
- Robust simulations (including solver behaviour) for **3D poromechanical model** with network of fractures.
- **Ongoing work**: extension to arbitrary order of approximation.
↪ **Ritesh's presentation, MS113, Friday 10am-12noon (Leacock 232)**



Funded by
the European Union



European Research Council
Established by the European Commission

Funded by the European Union (ERC Synergy, NEMESIS, project number 101115663). Views and opinions expressed are however those of the authors only and do not necessarily reflect those of the European Union or the European Research Council Executive Agency. Neither the European Union nor the granting authority can be held responsible for them.

Thank you for your attention!